

Addressing Key Challenges of Adversarial Attacks and Defenses in the Tabular Domain: A Methodological Framework for Coherence and Consistency

Yael Itzhakev^{a,*}, Amit Giloni^a, Yuval Elovici^a and Asaf Shabtai^a

^aDepartment of Software and Information Systems Engineering, Ben-Gurion University of the Negev, Beer-Sheva, 8410501, Israel

ARTICLE INFO

Keywords:

Tabular data
Adversarial attacks
Anomaly detection
Machine learning
Security
XAI

ABSTRACT

Machine learning models trained on tabular data are vulnerable to adversarial attacks, even in realistic scenarios where attackers only have access to the model's outputs. Since tabular data contains complex interdependencies among features, it presents a unique challenge for adversarial samples which must maintain coherence and respect these interdependencies to remain indistinguishable from benign data. Moreover, existing attack evaluation metrics—such as the success rate, perturbation magnitude, and query count—fail to account for this challenge. To address those gaps, we propose a technique for perturbing dependent features while preserving sample coherence. In addition, we introduce Class-Specific Anomaly Detection (CSAD), an effective novel anomaly detection approach, along with concrete metrics for assessing the quality of tabular adversarial attacks. CSAD evaluates adversarial samples relative to their predicted class distribution, rather than a broad benign distribution. It ensures that subtle adversarial perturbations, which may appear coherent in other classes, are correctly identified as anomalies. We integrate SHAP explainability techniques to detect inconsistencies in model decision-making, extending CSAD for SHAP-based anomaly detection. Our evaluation incorporates both anomaly detection rates with SHAP-based assessments to provide a more comprehensive measure of adversarial sample quality. We evaluate various attack strategies, examining black-box query-based and transferability-based gradient attacks across four target models. Experiments on benchmark tabular datasets reveal key differences in the attacker's risk and effort and attack quality, offering insights into the strengths, limitations, and trade-offs faced by attackers and defenders. Our findings lay the groundwork for future research on adversarial attacks and defense development in the tabular domain.

1. Introduction

Machine learning (ML) models trained on tabular data are widely deployed in diverse industry sectors including finance (e.g., for computing credit risk) [12, 37], healthcare (e.g., for analyzing administrative claims and patient registry data) [13], and energy (e.g., for predicting energy and electricity consumption) [30, 43]. However, recent research has highlighted their vulnerability to adversarial attacks, in which malicious data samples are used to mislead the model into producing incorrect outputs [2, 8, 36, 21]. For instance, an applicant may slightly increase their reported income (influencing the “income level” feature), crossing a decision threshold and thereby changing the model's decision from ‘reject’ to ‘approve.’ Such adversarial attacks can even be conducted in realistic black-box settings, where the attacker has no knowledge of the model's internals and can only query the model to receive outputs.

While extensive research has been performed in the image [50, 52, 26, 42], audio [31], text [50, 35, 20], and graph data [50, 46] domains, the tabular domain remains relatively underexplored. This paper addresses several key challenges in the realm of adversarial attacks, focusing on tabular data.

Crafting Coherent and Consistent Adversarial Samples:

Crafting adversarial samples in the tabular domain presents unique challenges compared to other data types. Unlike domains such as images, audio, and text, which contain homogeneous feature types with well-defined dependencies (spatial in images, temporal in audio, and semantic in text), the tabular domain is characterized by heterogeneous feature types, diverse data constraints, and complex interdependencies. Correlations in tabular data can also be complicated. For instance, in a loan dataset, a high credit score strongly correlates with approval, but for a low credit score, approval depends on other factors like income or debt, making the correlation conditional.

Models trained on tabular data often rely on interdependent features, where the values of some features (dependent features) are influenced by others (influencing features). Therefore, in adversarial attacks, perturbations to dependent features must align with the influencing features to preserve these constraints and interdependencies, maintaining coherence and consistency to avoid detection. For instance, the BMI is derived from height and weight, so when altering these influencing features (such as height or weight) during an attack, it is essential to ensure that the BMI value remains consistent with the changes.

Multiple dependent features further complicate the process of maintaining this alignment. Furthermore, while some dependencies are well-defined (as is the case with the BMI), others may be non-linear, indirect, or influenced by features

*Corresponding author

✉ freidiya@post.bgu.ac.il (Y. Itzhakev)

ORCID(s): 0009-0009-9854-8480 (Y. Itzhakev)

unknown to the attacker. For instance, the feature “employee performance rating,” used in a model predicting company efficiency, depends on factors such as project completion rate, peer feedback, client satisfaction scores, and overtime hours. In practice, the attacker may not have access to all influential features or know exactly how these features contribute to the employee performance rating. These complex, often domain-specific interdependencies and feature correlations make it much harder to maintain consistency and coherence when crafting adversarial samples in the tabular domain.

Evaluation Criteria for Distinguishable Adversarial

Samples: Existing evaluation methods for adversarial samples primarily focus on measuring the perturbation magnitude using L_p norms, which are intended to indicate the level of detectability (i.e., the risk that the attack will be exposed). However, in the context of tabular data, simply limiting perturbation magnitudes is insufficient. Effective adversarial attacks must ensure that samples remain coherent, consistent, and in-distribution to evade detection. While previous work has acknowledged these challenges (see Section 2.3), there is a lack of concrete evaluation methods for quantifying the distinguishability of adversarial samples in the tabular domain.

Empirical Analysis of Different Attack Strategies:

While adversarial attacks have been extensively studied in other domains, the analysis of black-box attack strategies in the tabular domain has been limited. Query-based and transferability-based are common black-box attack strategies.

In query-based attacks [8], it is assumed that the attacker has unlimited access to the target model’s predictions. By repeatedly querying the model, he attacker is able to iteratively optimize an adversarial example to induce misclassification. Transferability-based attacks [36, 21] operate under a more constrained threat model, where the attacker lacks direct access to the target model’s outputs but is assumed to have access to a large amount of reliable data to train an accurate surrogate model. In this case, the attacker optimizes the adversarial sample to mislead the *surrogate* model and then uses this sample to mislead the target model with a single query.

Adversarial attacks are used by both defenders and attackers both of whom may choose different attack strategies based on their goals, resources, and constraints. *Defenders* who are interested in assessing their model’s vulnerability often use adversarial attacks for automated penetration testing or adversarial training, which involves creating adversarial samples to improve the model’s robustness [11, 23]. Since defenders have full access to their model and can make unlimited queries, query-based attacks are a practical option. In contrast, *attackers* aiming to minimize the number of queries performed and avoid detection, might prefer transferability-based attacks that use gradient methods on neural networks, as they capture underlying feature interactions necessary for subtle perturbations. Understanding how and whether query-based attacks reflect other types of attacks, such as

transferability-based gradient attacks, is crucial when using them to improve model defenses.

In this paper, we aim to advance adversarial research in the tabular domain by addressing existing gaps in the literature. We compare the effectiveness of various attack strategies against classification models to provide insights for both attackers and defenders. Additionally, we developed a novel technique for consistent perturbation of dependent features and concrete evaluation criteria for assessing attack quality. We perform a detailed examination of both black-box query- and transferability-based gradient attacks, tailored to respect tabular distribution constraints.

Our proposed technique for perturbing dependent features aims to address the challenge of crafting coherent and consistent adversarial samples. This technique uses *regression models* to correct dependent features during the attack process, ensuring that they maintain realistic relationships with interdependent features and remain consistent with the values of other features (see Section 3).

To assess the distinguishability and quality of adversarial samples (see Section 3), we introduce Class-Specific Anomaly Detection (CSAD), an approach that measures the anomaly detection rate of adversarial samples relative to the distribution of benign samples from the specific class predicted by the target model. CSAD leverage existing anomaly detection methods to detect anomalies when inconsistencies are present within class-specific distributions. Additionally, we propose complementary criteria that use explainability-based analysis to examine how adversarial samples influence the model’s decision-making process. This analysis uses SHapley Additive exPlanations (SHAP)[33], a widely adopted explainability (XAI) technique[3], to quantify the inconsistencies induced by adversarial perturbations in the model’s internal reasoning.

Our comparison of attack strategies’ performance factors integrates both traditional metrics of the attacker’s risk (success rate, query count, and L_p norms) and effort and the new evaluation criteria introduced in this paper (sample anomaly detection and feature importance consistency), providing a thorough assessment of adversarial sample quality and attack effectiveness.

Four different tree-based target models are used to explore and evaluate the attack strategies (process illustrated in Fig. 1) on three datasets: the Hateful Users on Twitter [44] and Intensive Care Unit [22] public datasets, which are benchmark datasets in the tabular domain, and the Video Transmission Quality (VideoTQ) dataset, which is a proprietary dataset. Seven attacks are examined in our evaluation: two well-known query-based attacks (the boundary and HopSkipJump attacks [6, 9] that can be adapted for tabular data [8]) and five transferability-based gradient attacks that varied in terms of their feature selection techniques (a basic attack [36] in which features were randomly selected and four attacks in which features were selected based on their importance [21]).

This work sheds light on the key trade-offs between these attacks for the tabular domain, which can guide the selection

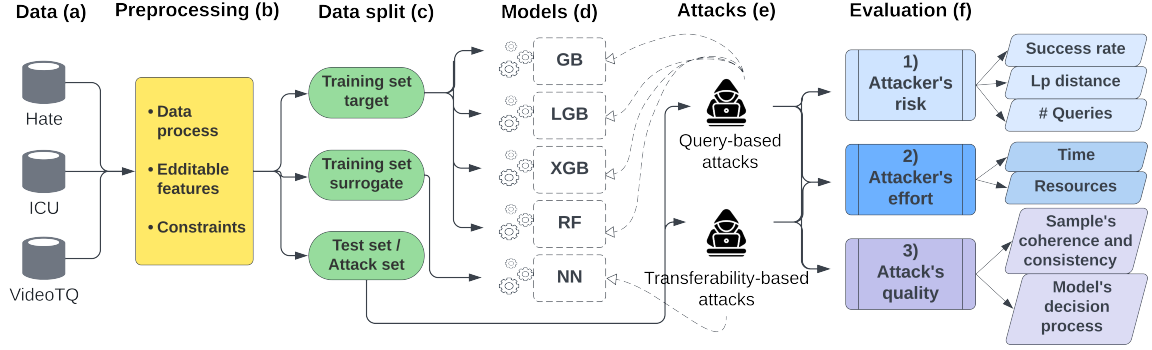


Figure 1: An overview of the paper's methodological framework.

of attack strategies and motivate the development of new defense approaches tailored to the unique properties of this domain.

The contributions of our work can be summarized as follows:

- We propose a novel technique for perturbing inter-dependent features in tabular data, leveraging regression models to preserve coherence and ensure feature consistency, overcoming a key challenge in tabular adversarial attacks.
- We introduce CSAD, an approach that assesses anomalies relative to class-specific distributions rather than global thresholds, which improve sensitivity to inconsistencies among features.
- We developed comprehensive dual evaluation criteria based on anomaly detection assessment of the sample values and feature importance, providing a core principled framework to quantify both the quality of tabular adversarial examples and their impact on model decision-making.
- To the best of our knowledge, this study is the first to systematically compare adversarial attack strategies' performance factors in the tabular domain, providing critical insights into their effectiveness, limitations, and corresponding defense strategies.
- The resources of this study (preprocessed data, code, models, and adversarial samples) will be made publicly available to promote future research and reproducibility.

The remainder of this paper is organized as follows: In Section 2, we discuss related work. Section 3 introduces our methodological framework, followed by Section 4 and Section 5, which present the experimental setup and provide a thorough analysis of the examined query- and transferability-based attack behavior. Finally, Section 6 and Section 7 conclude with insights for attackers and defenders within tabular data domains.

2. Background and Related Work

2.1. State-of-the-Art Adversarial Attacks in Tabular Data Domains

Szegedy *et al.* [47] introduced the concept of an adversarial attack in which an attacker provides a malicious data sample aimed at misleading the ML model and causing it to produce incorrect output. Their adversarial sample was crafted by performing subtle changes to an image, which were imperceptible to the human eye but misled the target model. However, research conducted in tabular subdomains, such as fraud detection and recommendation systems [2, 8, 14], has highlighted additional critical challenges within the tabular domain. These challenges include the constraints of editable and non-editable features (e.g., ID, date of birth), data imbalance, and the presence of noncontinuous features (e.g., categorical features). The authors of these studies also mentioned the complexity of perturbing discrete values while maintaining the semantic integrity of the sample, as well as capturing nuances when designing attacks. This discussion was further elaborated on in [36].

Most recent adversarial attacks were demonstrated under black-box conditions (i.e., the attacker has no prior knowledge of the target model and only has the ability to query it [34]). The main types of black-box attacks are query-based attacks and transferability-based attacks.

In query-based attacks, the attacker assumes that the target model can be queried multiple times, and when queried, the attacker receives the model's confidence or classification. The attacker iteratively adjusts the sample's values, based on the model's output, until the optimization objective is fulfilled - the target model is misled and produces the desired output. Decision-based attacks are examples of black-box query-based attacks [7]. These attacks typically involve making a large initial modification to the original sample, such that the target model produces an incorrect prediction. Then the attacker optimizes the modified sample's values so they are as close as possible to the original sample while still misleading the target model. For evaluation, we implemented two decision-based attacks: The boundary attack and the HopSkipJump attack, which differ in terms of the extent of the initial changes made to the sample and

the optimization process performed [6, 9]. Modifications to these decision-based attacks for incorporating tabular data validity and editability constraints were made by [8].

In transferability-based attacks, the attacker trains a surrogate model, crafts an adversarial sample using a white-box attack on the surrogate model, and then utilizes the adversarial sample crafted to attack the target model in a single query [39].

An untargeted, transferability-based gradient attack designed to address tabular constraints was introduced in previous work [36, 21]. This architecture is based on NN and incorporates an embedding function to preserve feature correlations and ensure value consistency by minimizing L_2 distance and adjusting correlated features. The attack process iteratively perturbs features to reduce L_0 (i.e., the number of modified features) while applying validity and editability constraints, demonstrating its applicability in real-world scenarios. Another work [25] introduced a transferability-based attack that considers feature distribution in the perturbation process, addressing the tabular distribution challenge while excluding validity constraints.

2.2. Existing Methods for Evaluating Adversarial Attacks

Commonly used metrics for assessing the performance of adversarial attacks include:

1. **Attacker’s risk.** The attacker’s risk is assessed by the attack success rate [19, 2], the number of queries made to the target model [24, 48], and the extent to which the adversarial sample has been distorted, consequently becoming distinguishable. The distortion is typically measured using L_p norms such as L_0 , L_2 , and L_∞ , which quantify the magnitude of perturbations applied to the original samples [19, 29, 15, 2, 36, 21], and can also be evaluated by computing the average error between the original sample and the corresponding adversarial samples [18].
2. **Attacker’s effort.** The attacker’s effort is assessed by the time required to create the adversarial sample, as well as the amount of data and time needed to train the surrogate model [1].

2.3. Indistinguishability in the Tabular Domain

While most metrics used to assess the attacker’s effort and risk are consistent across various domains including tabular data, the detectability dimension of adversarial samples should be measured differently for tabular data domains. In the computer vision domain, for example, an adversarial sample is considered to be indistinguishable if the human eye is unable to recognize the difference between the adversarial sample and the original sample [47, 19, 40, 29]. It is commonly assessed by measuring the distance between the original and perturbed images using L_2 norm.

However, in the tabular domain, “human eye” inspection is less meaningful, as only domain experts can accurately examine such differences [2, 8]. Furthermore, when looking at

tabular data samples, a domain expert would “select” a limited number of features to examine and determine whether the sample is real or manipulated by an adversary [2] based on those features. Given the above, the authors of [2, 8] proposed evaluating the distinguishability of a tabular adversarial sample based on the number of “important” features (i.e., features that a domain expert would likely examine) altered in the adversarial attack. Accordingly, an adversarial sample is considered more perceptible as the number of changes in important features increases. However, this evaluation method is neither objective nor practical, as it requires a domain expert to manually assess each sample individually. Moreover, it does not consider the fact that altering even a small number of features can cause inconsistency with the rest of the sample, making it distinguishable from the benign data distribution and detectable by anomaly-based methods.

Prior research highlighted the significance of both consistency [36, 25] and validity [36, 18] when analyzing the quality of adversarial samples. Validity can be assessed by examining whether each feature value falls within a valid range [2, 36] and by measuring the sample’s deviation from the distribution of benign data [36]. However, no concrete metric has been used to quantify the coherence and consistency of adversarial samples, which are influenced by complex correlations between feature values [36].

We address this gap by proposing two criteria that assess the distinguishability of adversarial samples from benign ones using an “anomaly detection rate,” which provides an indirect evaluation of their coherence and consistency. We assume that adversarial samples lacking structural coherence or consistency with the benign data distribution are more likely to exhibit anomalies, making them both distinguishable and detectable.

Although there are many well-established anomaly detection techniques for the image domain, not all of them are directly applicable to tabular data. Since some methods fail to fully capture multivariate dependencies, selecting the right approach is crucial. Methods such as convolutional autoencoders (AEs) and generative adversarial networks (GANs) leverage spatial correlations but often struggle to capture the complex dependencies found in tabular data and therefore should be modified for the tabular domain [4]. Similarly, traditional statistical techniques like t-tests and the ANOVA assume normality and independence [16], limiting their ability to detect anomalies in the tabular domain where variables might not follow normal distributions and the relationships between variables are often complex and non-linear. Other simple approaches, such as Z-score thresholding, focus on individual feature deviations but fail to account for multivariate dependencies. Additionally, some commonly used anomaly detection techniques have inherent limitations for tabular data. For instance, PCA-based methods assume linear relationships, limiting their effectiveness in detecting non-linear dependencies in high-dimensional datasets [45].

More suitable approaches for tabular data include AEs, which learn latent representations to detect deviations from

expected patterns [45], and the isolation forest (IF) algorithm, which identifies anomalies by isolating points in a partitioned feature space. However, while effective for detecting extreme outliers, this algorithm is less sensitive to subtle structural inconsistencies [51].

3. Methodological Framework for Addressing Challenges in Adversarial Attacks and Evaluation in the Tabular Domain

In this section, we introduce the black-box query- and transferability-based attacks evaluated, along with the modifications made in order to deal with the tabular constraints. We also present our novel technique for perturbing dependent features, as well as two criteria for evaluating the quality of adversarial attack samples. These criteria focus on the distinguishability of the adversarial samples and their impact on the target model’s internal behavior in the tabular domain.

3.1. Modifying Adversarial Attacks to Address Tabular Constraints.

In our evaluation (see Section 4.5), we examined two decision-based attacks: the boundary attack [6] and the HopSkipJump attack [9], which were adjusted to address tabular constraints and evaluated by [8]. We implemented these attacks by applying additional constraints based on feature distributions (e.g., limiting values according to statistical information) and making adjustments to ensure validity (e.g., [0,1] values for binary features and ordinal values for categorical features) and editability (guided by domain knowledge).

In addition, we performed transferability-based gradient attacks based on the architecture proposed in [36, 21], which is a sophisticated attack designed to craft valid and consistent adversarial samples.

The details and pseudocode for the boundary and HopSkipJump attacks, as well as the transferability-based attacks, adapted to take into account the constraints of tabular data, are provided in Appendix A.

3.2. Perturbing Dependent Features.

To ensure coherence and maintain feature consistency when crafting adversarial samples, we introduce a novel technique for perturbing dependent features. Specifically, for each dependent feature, we train a regression model on the benign samples, excluding the target feature. This model then predicts the value of the dependent feature based on the values of the other features in the sample.

During the adversarial attack process, when perturbations are applied to features, the regression model corresponding to each dependent feature is queried to predict its value, ensuring that the dependent feature remains consistent with the rest of the sample. This approach ensures that the perturbations respect indirect dependencies between features, thereby maintaining the overall coherence of the sample.

In our implementation of both query- and transferability-based attack strategies, the attack process includes an additional step in which the dependent features, as identified by domain knowledge, are adjusted according to the predictions from the regression models. This step helps maintain feature consistency and reduces the likelihood of generating detectable anomalies.

3.3. Evaluating the Quality of Adversarial Attacks

The quality of an adversarial attack is measured by its ability to evade detection, which depends on how well the crafted samples maintain coherence and consistency with benign data. To assess this, we propose two evaluation criteria:

1. Feature Space Coherency – Quantifying the distinguishability of adversarial samples from benign data distributions.
2. Model Interpretation Stability – Analyzing the extent to which adversarial samples influence the internal decision-making process of the target model when queried.

Both criteria leverage a key contribution of our work: the introduction of Class-Specific Anomaly Detection (CSAD). Unlike traditional one-class anomaly detection methods that assume all benign samples belong to a single class or distribution, CSAD evaluates anomalies relative to the specific class to which the adversarial sample is assigned by the target model. This class-aware evaluation enables CSAD to account for class-dependent variations in benign data, resulting in more effective anomaly detection.

The CSAD Approach. In the CSAD approach, we evaluate anomalies **separately** for each target class. For instance, given a dataset with three classes, we train three distinct anomaly detection models—one for each class. Each model is trained exclusively on benign samples from its respective class, ensuring that the unique statistical properties of each class-specific distribution are captured. When an adversarial sample is generated, it is evaluated using the anomaly detection model corresponding to its **predicted class**. For example, if an adversarial sample is classified as class 1 by the target model, it is assessed using the anomaly detection model trained on benign samples from class 1.

This approach addresses a key limitation of traditional anomaly detection techniques, where adversarial samples appear anomalous within the general data distribution, but not within their assigned class. Adversarial attacks introduce subtle perturbations that might preserve the statistical characteristics of the **original** sample while misleading the model. By design, adversarial samples can still resemble their true class and remain indistinguishable from other benign samples in that class. However, when analyzed in the context of the **target class** (the class to which they are misclassified), these perturbations may exhibit distinct anomalies. By leveraging class-specific distributions, CSAD enables more precise differentiation between adversarial and benign samples, capturing anomalies that would otherwise go undetected.

Feature Space Coherency. To evaluate the distinguishability of adversarial samples, we propose measuring the anomaly detection rate—the percentage of samples identified as anomalies for each attack. The anomaly detection rate metric serves as an indicator of how different adversarial samples are from the benign data distribution. We compute the anomaly detection rate using two well-established methods from the anomaly detection domain: *i)* Isolation Forest (IF) – A tree-based algorithm that identifies anomalies based on how easily a sample can be isolated in a feature space, and *ii)* Autoencoder (AE) – A neural network-based model that reconstructs benign samples and detects anomalies based on the reconstruction error.

In the IF algorithm, a sample is considered anomalous if it is classified as an outlier. In the AE model, an anomaly is identified when its reconstruction error exceeds a threshold, defined in Eq. (1):

$$\text{Threshold}(x_c, AE_c) = \text{mean}(\text{test}_{c,r,\text{error}}) + 0.5 * \text{std}(\text{test}_{c,r,\text{error}}) \quad (1)$$

where x_c is a sample classified as class c , AE_c is the autoencoder trained on benign samples of class c , and $\text{test}_{c,r,\text{error}}$ represents the reconstruction error on a validation set of class c during the AE’s training.

The AE model consists of an embedding layer with 64 neurons, and it was trained using the Adam optimizer with a learning rate of $1e-3$, a weight decay of $1e-8$, for 10 epochs, and the mean square error (MSE) as the loss. The IF method was implemented with 100 estimators and *max_features* set to one, without bootstrapping. For comparison, the contamination parameter in the IF model was set to match the false positive rate (FPR) obtained by the AE according to the threshold defined in Eq. (1), corresponding to the proportion of benign samples with a reconstruction error above this threshold.

Other anomaly detection methods can be considered depending on the dataset characteristics and attack patterns.

Model Interpretation Stability. In addition to measuring distinguishability, we assess how adversarial samples influence the target model’s decision-making process. Adversarial perturbations may alter the model’s perception of feature importance, leading to inconsistencies in the model’s reasoning. To quantify this effect, we employ SHAP [33], a widely used explainability technique that provides a unified measure of feature importance in ML models. SHAP estimates each feature’s contribution to a prediction by comparing actual predictions with averages across all possible feature combinations.

We introduce two metrics based on SHAP: (1) Importance-Based Anomaly Detection Rate – The percentage of adversarial samples where at least one feature’s SHAP value falls outside the range observed in benign samples, and (2) Average Anomalous SHAP Features per Sample – The average number of features in an adversarial sample with SHAP values outside the benign distribution. Lower values for these metrics indicate higher-quality adversarial samples,

as they remain consistent with the model’s internal reasoning despite altering predictions.

Importantly, CSAD is also being extended to SHAP-based anomaly detection; since we assess traditional anomaly detection methods per class, we compute SHAP-based anomalies within the context of each class. This ensures that SHAP value deviations are analyzed relative to the specific class distribution, rather than across the entire dataset. The SHAP values were extracted using SHAP Tree-Explainer.

Leveraging Anomaly Detection for Defense. The Importance-Based Anomaly Detection Rate and Average Anomalous SHAP Features per Sample methodologies not only assess adversarial quality but also serve as defense mechanisms. Since adversarial samples often exhibit statistical or interpretability inconsistencies, the anomaly detection rate—whether computed directly or through SHAP values—serves as a robust indicator for detecting adversarial attacks. Our class-specific approach further enhances the ability to distinguish between benign and adversarial samples, offering a stronger defense against adversarial manipulation.

4. Experimental Setup

4.1. Research Questions

In this study, we address the following research questions regarding the tabular domain:

- **RQ#1** To what extent do query-based attacks reflect the behavior of transferability-based gradient attacks?
- **RQ#2** How the perturbed samples of different attack strategies differ in terms of the attacker’s risk and effort?
- **RQ#3** Is the model’s decision-making process aligned according to the samples’ SHAP values for both a benign samples and perturbed samples?

4.2. Datasets

We conducted our evaluation on two publicly available, real-life tabular datasets and an additional proprietary tabular dataset. These datasets contain a relatively large number of samples and features, as well as a variety of feature types, to ensure robust and reliable results.

1. *The Hateful Users on Twitter (Hate) dataset* [44]. This dataset contains 4,971 records of English-speaking Twitter users that were manually annotated as hateful or non-hateful users. This dataset is unbalanced and includes 544 records from class 1 (i.e., hateful users). The dataset comprises 115 numerical and categorical features, with 109 of them being mutable (i.e., can be changed by the attacker).
2. *Intensive Care Unit (ICU) dataset*¹ [22]. This dataset, which contains the medical records of 83,978 patients

¹ICU:kaggle.com/competitions/widsdatathon2020/data

who were admitted to the intensive care unit, is used to predict the mortality of the patients. The dataset is unbalanced and includes 7,915 records from class 1 (i.e., patients who died while in the ICU). The dataset comprises 74 numerical and categorical features, 45 of which are mutable and five of which contain values that are dependent on other features.

3. *Video Transmission Quality (VideoTQ) dataset.* This proprietary commercial dataset was obtained from RADCOM², a company specializing in service assurance for telecom operators, and it contains records of 54,825 streaming service media broadcasts. This dataset is used to predict a transmission’s resolution (i.e., high or low resolution). The dataset is unbalanced and includes 10,000 records from class 1 (i.e., high resolution). The dataset comprises 23 numerical and categorical features, nine of which are mutable.

4.3. Dataset Preprocessing

The preprocessing performed on each dataset (illustrated in Fig. 1 (b)) differs according to its characteristics, with the aim of creating highly accurate target models that are based on multiple features’ importance in the model’s decision-making process.

Hate dataset. In the preprocessing performed on the Hate dataset, we followed the preprocessing methodology outlined by Kaggle³. We also performed additional preprocessing steps, including removing the ‘user_id’ feature, systematically eliminating outliers, dropping features with a correlation exceeding 90%, and excluding instances with more than 80% missing data. In addition, features for which over 75% of the values were the same were removed.

We also performed label encoding on the binary and categorical features and filled in missing values by employing a regression model to predict the values for each feature. Additionally, features that contain the GloVe representations [41] of other features (which include ‘glove’ in their names) were removed, resulting in a distilled set of 311 features. To ensure that only meaningful and important features were used, we trained four models on the dataset (XGBoost [10], GradientBoost [17], LightGBM [27], and random forest [5]) and selected the top-40 important features for each model; the importance of all of these features exceeded 0.0001. The resulting dataset contains 115 features and 4,971 samples.

ICU dataset. In the preprocessing performed on the ICU dataset, we followed the preprocessing methodology outlined by Kaggle⁴. We also performed additional preprocessing, removing outliers, eliminating highly correlated features (with over 90% correlation), and excluding instances with over 80% missing values. In addition, features for which over 75% of the values were the same were removed. Samples for which the ‘bmi’ feature was missing, values were filled in by using the BMI formula based on the values in the ‘height’ and ‘weight’ features. For other features,

we filled in missing values by using a regression model to predict the values for each feature. Categorical features were label-encoded, and missing values were filled in by using the median feature value.

VideoTQ dataset. In the preprocessing performed on the VideoTQ dataset, we removed 15 records that had missing values, and eliminated outliers and highly correlated features (with over 90% correlation). Categorical features were label-encoded, and all timestamps were converted into separate date and time formats.

For all datasets, the editable and immutable features were determined and selected by a domain expert. All datasets were split into training and test sets, with 75% of the samples serving as the training set. Oversampling was performed by duplicating the training set samples in class 1 to address the significant class imbalance in the datasets. The oversampled training set was split into a target training set and a surrogate training set (for the attacker’s use in the transferability-based attacks). The test set is also used to create adversarial samples (i.e., the attack set) as illustrated in Fig. 1 (c) and further detailed in Section 4.8.

4.4. Target Models

For our evaluation, we trained four different ML target models: XGBoost [10] (XGB), GradientBoost [17] (GB), LightGBM [27] (LGB), and random forest [5] (RF) (see 1 (d)). The hyperparameters used to train the models were fine-tuned, and therefore varied across different training sets. The XGBoost target models were trained using 90, 70, and 300 estimators; a max depth of 3, 8, and 5; and a learning rate of 1, 0.1, and 1 for the Hate, ICU, and VideoTQ datasets respectively. The GradientBoost target models were trained using 40, 500, and 300 estimators; a max depth of 7, 6, and 5; and a learning rate of 2.5, 0.01, and 1 for the Hate, ICU, and VideoTQ datasets respectively. The LightGBM target models were trained using 300, 200, and 200 estimators; a max depth of 7, 8, and 8; and a learning rate of 1, 0.1, and 0.1 for the Hate, ICU, and VideoTQ datasets respectively. The random forest target models were trained using 100, 500, and 500 estimators and a max depth of 4, 9, and 9 for the Hate, ICU, and VideoTQ datasets respectively.

4.5. Attack Configuration

In our comparison of different types of attacks, we used two query-based attacks and five transferability-based gradient attacks that varied in terms of their feature selection techniques. The boundary attack was performed with an epsilon of one, a delta of one, maximal iterations of 3000, the number of trials set at 20, and an adaptation step of one. The HopSkipJump attack was performed with the L2 norm, maximal iterations of 50, the max-eval parameter set at 10,000, the init-eval set at 500, and an init size of 100. The parameters of the boundary and HopSkipJump attacks were identical for all datasets, except for the maximal iteration number; for the VideoTQ dataset this was set at 1000 in the HopSkipJump attack.

The transferability-based attacks require the attacker to train a surrogate model (illustrated in Fig. 1 (d, e)). In

²radcom.com/

³kaggle.com/code/binaicrai/fork-of-fork-of-wids-lgbm-gs

⁴kaggle.com/code/binaicrai/fork-of-fork-of-wids-lgbm-gs

our evaluation, all surrogate models were neural networks, and we used an embedding layer to try to maintain the consistency of the crafted samples, following the approach employed in other studies [36, 21]. All surrogate models were comprised of two components: a sub-model for embedding and a sub-model for classification, both of which were fine-tuned for optimized performance. The embedding sub-model had an input size matching the number of features in the input sample, followed by a dense layer with 256 neurons and ReLU and PReLU activations for the Hate and VideoTQ datasets respectively. For the ICU dataset, the embedding sub-model had three dense layers with 256, 128, and 64 neurons and ReLU activation for all layers. The output size of all embedding sub-models was set at 16, i.e., the embedding size. The classification sub-model had a dense layer with 16 neurons (matching the embedding size) with ReLU activation for the Hate and ICU datasets and PReLU activation for the VideoTQ datasets. This was followed by a dropout layer with a dropout rate of 0.1. All surrogate models were trained using the binary cross-entropy loss function [32] and the Adam optimizer [28] with a learning rate of 0.2 for the Hate and VideoTQ datasets and 0.1 for the ICU dataset.

After training, the attacker performs the adversarial attack against the surrogate model by perturbing a group of features in each iteration. Each transferability-based attack employs a different feature selection technique to determine which features to perturb (see Appendix A).

For importance-based selection technique, the k most important features are selected, along with the n features most correlated with them—resulting in a total of $k \times n$ additional perturbed features per iteration. In each subsequent iteration, the next k most important features and their n most correlated features are added to the set of perturbed features. This process continues until an adversarial sample is found or no additional features remain for selection. Feature importance is determined using XGBoost, gradient boosting, LightGBM, and random forest models, each trained separately for this purpose. For random-based selection attacks, k features are randomly chosen in each iteration, along with their n most correlated features.

For all attacks, k was set at two and n was set at one (i.e., one correlated feature per selected feature). The correlated features were identified using the Pearson correlation coefficient [49].

4.6. Regression Models

Of the datasets used in our evaluation, the ICU dataset is the only one containing dependent features whose dependencies are not well-defined. Specifically, these dependent features are: ‘*apache_3j_bodysystem*,’ ‘*apache_3j_diagnosis*,’ ‘*d1_mbp_invasive_max*,’ and ‘*d1_mbp_invasive_min*.’

The regression models were trained on the dataset used to train the surrogate models, using 200 estimators, a max depth of six, and a learning rate of 0.1 for the ‘*apache_3j_bodysystem*’ and ‘*apache_3j_diagnosis*’

features, and 0.01 for the ‘*d1_mbp_invasive_max*’ and ‘*d1_mbp_invasive_min*’ features.

4.7. Threat Model

We assume that the attacker can query the target model and has an unlimited query budget for query-based attacks and a query budget of one for transferability-based attacks; in each query to the target model, the attacker obtains the confidence score for the prediction. In addition, we assume that the attacker has no prior knowledge about the specific model architecture or ML algorithm used. The attacker also has no access to the internal parameters of the model (such as weights and biases) and cannot calculate any gradients related to the model. Furthermore, the attacker does not have access to the target model’s training data; however, we assume that the attacker has a surrogate dataset derived from the same distribution, meaning that it contains the same features, in the same order, as the training data.

4.8. Evaluation Setup

To ensure a robust evaluation, we created the attack set by filtering the test set to include only samples correctly classified by both the target and surrogate models, excluding those already misclassified. This filtering retained 85%, 69%, and 91% of samples from the Hate, ICU, and VideoTQ datasets, respectively. Next, we randomly selected a balanced number of samples from each class. As a result, the attack sets contained 182, 1,000, and 1,000 samples for the Hate, ICU, and VideoTQ datasets, respectively. Our analysis of adversarial samples (using L_p norms or quality assessment), considered only samples that successfully fooled the target model (or both the surrogate and target models in the case of transferability-based attacks).

4.9. Evaluation Metrics

The main objective of our evaluation is to analyze the characteristics of and differences between black-box query- and transferability-based adversarial attacks with respect to three key factors: the attacker’s risk, the attacker’s effort, and the attack quality (illustrated in Fig. 1(f)). To perform a thorough analysis, we used the evaluation metrics commonly used in the literature and the metrics proposed in this work.

To assess the **attacker’s risk** we used three metrics (illustrated in Fig. 1(f-1)): *i*) the percentage of samples that successfully misled the model (attack *success rate*); *ii*) the average number of modified features (L_0) which might influence the attack’s ability to be successfully performed in real-life tabular data domains (due to the possible cost of changing the features), and the average Euclidean distance between the original and adversarial samples (L_2); and *iii*) the average number of queries required.

To assess the **attacker’s effort** we used three metrics (illustrated in Fig. 1(f-2)): *i*) the time it took to craft an adversarial sample; *ii*) the number of data samples needed to execute the attack; and *iii*) the memory resources and computing capabilities required to craft the adversarial sample and perform the optimization process.

Table 1

Target and surrogate models’ performance on the test set.

Dataset	Metric	Models				
		GB	LGB	XGB	RF	Surrogate
Hate	Accuracy	0.91	0.92	0.88	0.91	0.95
	F1 Score	0.91	0.92	0.87	0.91	0.95
	Precision	0.93	0.94	0.94	0.89	0.92
	Recall	0.89	0.91	0.82	0.92	1.00
ICU	Accuracy	0.80	0.80	0.77	0.78	0.78
	F1 Score	0.79	0.81	0.75	0.77	0.79
	Precision	0.82	0.84	0.82	0.81	0.81
	Recall	0.77	0.74	0.69	0.74	0.74
VideoTQ	Accuracy	0.98	0.99	0.98	0.98	0.96
	F1 Score	0.99	1.00	0.99	0.99	0.97
	Precision	0.91	0.97	0.96	0.93	0.86
	Recall	0.98	0.99	0.96	0.98	0.93

The **attack quality** is reflected in the crafted adversarial sample, which were assessed using three metrics (illustrated in Fig. 1(f-3)): *i*) the *anomaly detection rate* of adversarial samples compared to benign samples, using IF and AE models, where a higher rate indicates less consistency and coherence; *ii*) the percentage of samples with at least one feature with an anomalous SHAP value (*Importance-Based Anomaly Detection Rate*); and *iii*) the average anomalous SHAP features per sample.

In all three metrics, a lower number is better as higher values indicates an abnormal influence on the model’s decision-making process. Each experiment was conducted separately for each target model, as SHAP values vary across models.

4.10. Experimental Environment Setup

All experiments were performed on an Intel Core i7-10700 CPU at 2.90 GHz processor with the Windows 10 Pro operating system, an Intel UHD Graphics 630 graphics card, and 32 GB of memory. The code used in the experiments was written using Python 3.10.9 and the following Python packages: PyTorch 2.0.0, adversarial-robustness-toolbox 1.13.0 [38], pandas 1.5.2, NumPy 1.23.5, TensorFlow 2.10.0, and Keras 2.10.0.

5. Experimental Results

5.1. Models’ Performance

Table 1 summarizes the performance of all target and surrogate models examined, presenting the accuracy, F1 score, precision, and recall values obtained by each model on the test set. As can be seen, all models were high-performing. The target models for the Hate dataset obtained accuracy values ranging from [88% – 91%], F1 scores ranging from [87% – 92%], precision values ranging from [89% – 94%], and recall values ranging from [82% – 92%]. The target models for the ICU dataset obtained accuracy values ranging from [77% – 80%], F1 scores ranging from [75% – 81%], precision values ranging from [81% – 84%], and recall values

ranging from [69%–77%]. The target models for the VideoTQ dataset obtained accuracy values ranging from [98% – 99%], F1 scores ranging from [99% – 100%], precision values ranging from [91% – 97%], and recall values ranging from [96%–99%].

5.2. Attacker’s Risk

Tables 2 and 3 and Fig. 2 present the results for the attacker’s risk metrics (see Section 4.9) for the query- and transferability-based attacks performed against different target models on each dataset.

Table 2 presents details on the following attack success rates: Target Success Rate (SR): The percentage of adversarial samples that successfully mislead the target model; Surrogate Success Rate (Surrogate SR): The percentage of adversarial samples that successfully mislead the surrogate model; Transfer Success Rate (Transfer SR): The percentage of adversarial samples that successfully transfer from the surrogate model to the target model, calculated as the ratio of the Surrogate SR. Overall Success Rate (Overall SR): The percentage of adversarial samples that successfully mislead both the surrogate and target models, computed as the ratio of the entire attack set.

As detailed in Table 2, the query-based attacks have consistently high success rates (SR) on all target models across the Hate and ICU datasets. For example, on the Hate and ICU datasets, both attacks achieve success rates ranging between [98% – 100%] across all target models. In comparison, the success rate varies more for the transferability-based attacks. The success of these attacks relies on the performance of the surrogate models and the transferability of adversarial samples. For instance, on the Hate dataset, despite successfully fooling surrogate models in 98.9% of cases, the transferability-based attacks demonstrated limited effect on the target models, with success rates falling below 12% when employing random feature selection (Transfer random). However, when using importance-based feature selection (Transfer imp.), the success rates improved, ranging between [20% – 86%]. A similar phenomenon can be observed on the ICU dataset, where transferability-based attacks continued to perform variably, depending on the feature selection method employed. On the VideoTQ dataset, unlike the other datasets, transferability-based attacks had more consistent performance, achieving a ~50% success rate overall. In contrast, the query-based attacks displayed more variability, with success rates ranging between [65.9% – 82.6%] for the boundary attack and between [50% – 67.9%] for the HopSkipJump attack.

Table 3 presents the average number of queries required to generate adversarial samples for query-based attacks. As can be seen, the examined query-based attacks require a significant number of queries, ranging from hundreds to hundreds of thousands. In contrast, transferability-based attacks require just a single query for all datasets.

Fig. 2 illustrates the distribution of both the number of modified features (L_0) and the Euclidean distance (L_2) between the adversarial attacks and the original samples.

Table 2

Attacker's risk: performance of query- and transferability-based attacks on different target models, evaluated using the following metrics: Target Success Rate (*SR*): percentage of adversarial samples that successfully mislead the target model; Surrogate Success Rate (*Surrogate SR*): percentage of adversarial samples that successfully mislead the surrogate model; Transfer Success Rate (*Transfer SR*): percentage of successful adversarial samples that transfer from the surrogate model to the target model (computed as the ratio of the Surrogate SR); Overall Success Rate (*Overall SR*): percentage of adversarial samples that mislead both the surrogate and target models (computed based on the entire attack set). Note that importance-based feature selection techniques are referred to as *Imp.* in the table.

Dataset	Target Model	Query Attacks		Transferability Attacks					
		boundary	HopSkipJump SR (%)	random	GB imp. Surrogate SR (%) / Transfer SR (%)	LGB imp. Surrogate SR (%) / Transfer SR (%)	XGB imp. Surrogate SR (%) / Transfer SR (%)	RF imp.	
Hate	GB	100	100	98.9 / 13.9 / 13.7	98.9 / 70.6 / 69.8	98.9 / 44.4 / 44.0	98.9 / 83.3 / 82.4	98.9 / 86.7 / 85.7	
	LGB	100	100	98.9 / 7.8 / 7.7	98.9 / 71.1 / 70.3	98.9 / 45.6 / 45.1	98.9 / 73.9 / 73.1	98.9 / 85.0 / 84.1	
	XGB	100	100	98.9 / 12.2 / 12.1	98.9 / 70.0 / 69.2	98.9 / 36.7 / 36.3	98.9 / 68.3 / 67.6	98.9 / 71.7 / 70.9	
	RF	100	100	98.9 / 2.8 / 2.7	98.9 / 36.7 / 36.3	98.9 / 20.6 / 20.3	98.9 / 54.4 / 53.8	98.9 / 73.3 / 72.5	
ICU	GB	98.6	98	87.4 / 9.4 / 8.2	87.8 / 45.4 / 39.9	87.4 / 25.4 / 22.2	88.6 / 41.9 / 37.1	88.4 / 45.8 / 40.5	
	LGB	98.7	97.9	87.4 / 12.8 / 11.2	87.8 / 35.8 / 31.4	87.4 / 29.1 / 25.4	88.6 / 34.2 / 30.3	88.4 / 36.4 / 32.2	
	XGB	99.9	98.2	87.4 / 24.5 / 21.4	87.8 / 55.2 / 48.5	87.4 / 41.3 / 36.1	88.6 / 50.5 / 44.7	88.4 / 55.3 / 48.9	
	LGB	99.2	99.2	87.4 / 11.4 / 10.0	87.8 / 44.9 / 39.4	87.4 / 18.4 / 16.1	88.6 / 42.8 / 37.9	88.4 / 45.4 / 40.1	
VideoTQ	GB	82.6	57.6	67.6 / 73.7 / 49.8	67.6 / 74.4 / 50.3	67.6 / 74.3 / 50.2	67.6 / 73.5 / 49.7	67.6 / 73.7 / 49.8	
	LGB	73.7	53	67.6 / 74.1 / 50.1	67.6 / 74.7 / 50.5	67.6 / 74.9 / 50.6	67.6 / 73.4 / 49.6	67.6 / 74.0 / 50.0	
	XGB	81.7	67.9	67.6 / 74.1 / 50.1	67.6 / 74.3 / 50.2	67.6 / 74.1 / 50.1	67.6 / 73.2 / 49.5	67.6 / 73.8 / 49.9	
	RF	65.9	50	67.6 / 74.0 / 50.0	67.6 / 74.0 / 50.0	67.6 / 74.0 / 50.0	67.6 / 74.0 / 50.0	67.6 / 74.0 / 50.0	

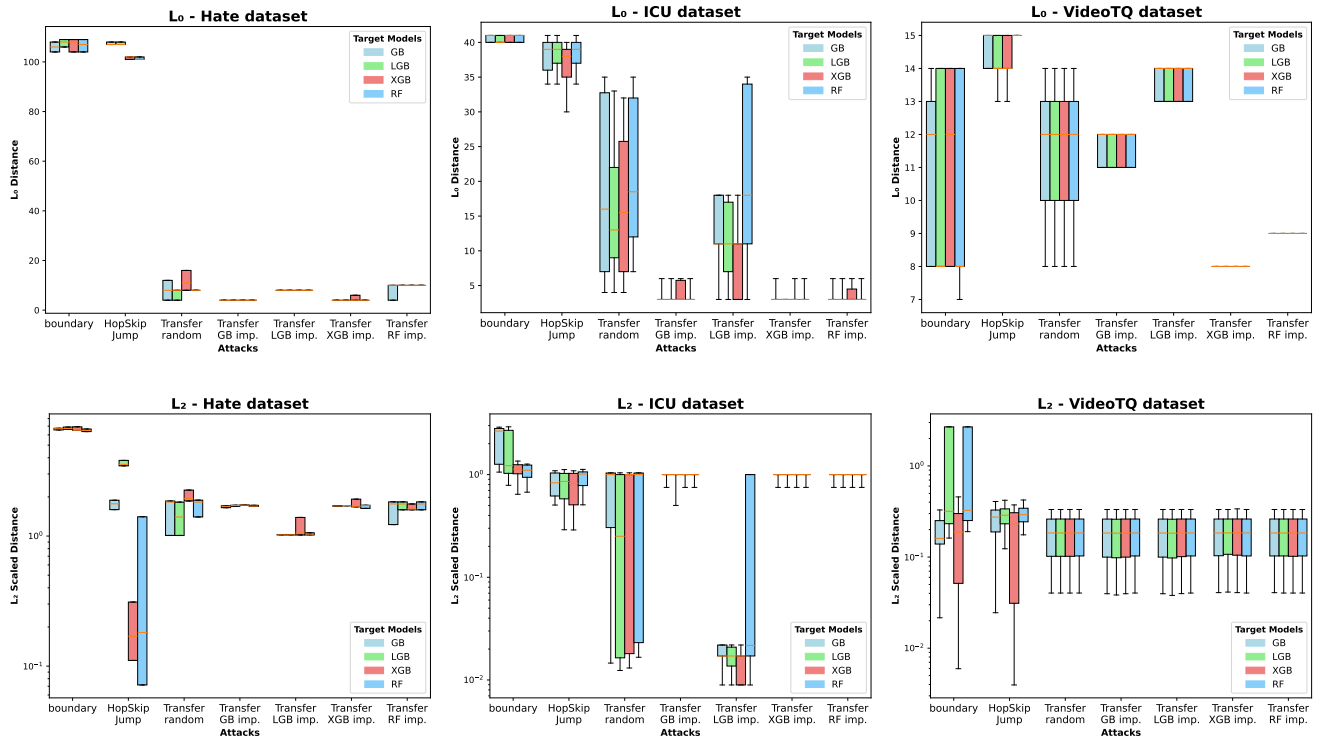


Figure 2: Attacker's risk: number of changed features (L_0 distance) and distortion size (L_2 distance), across query- and transferability-based attacks.

As can be seen in the figure, for most target models on the Hate and ICU datasets the examined query-based attacks consistently require more feature changes (i.e., larger L_0 distances) than the transferability-based attacks. For instance,

on the Hate dataset transferability-based attacks modify approximately 7 features, whereas query-based attacks modify around 103.

However, the VideoTQ dataset exhibits a less consistent pattern, with the boundary attack shows substantial variation in L_0 values, including samples with considerably lower L_0

Table 3

Attacker’s risk: average number of *queries* required to execute query-based attacks.

Dataset	Attack	Target Model			
		GB	LGB	XGB	RF
Hate	Boundary	292.5	302.0	275.4	309.8
	HopSkipJump	120260.0	120246.6	120243.4	120361.2
ICU	Boundary	902.3	2909.9	910.9	3531.7
	HopSkipJump	119231.3	119402.4	119642.7	121632.6
VideoTQ	Boundary	59604.1	57627.6	58860.6	60173.1
	HopSkipJump	16310.9	118374.4	103314.8	108680.1

distances than those of transferability-based attacks. This suggests that, in some cases, attacks required more feature modifications to succeed on this dataset.

In terms of L_2 distance, the two query-based attacks differ. Across the Hate and ICU datasets, the boundary attack generally causes larger distortions compared to transferability-based attacks. However, the VideoTQ dataset exhibits a different pattern: the boundary attack achieves notably lower L_2 distances on the GB and XGB target models than the transferability-based attacks. In contrast, while the HopSkipJump attack typically outperforms most transferability-based attacks by achieving lower median L_2 distances on most target models, it performs less effectively on the VideoTQ dataset, showing higher median L_2 distances on several target models.

In conclusion, while query-based attacks tend to achieve higher attack success rates, they have higher operational costs due to the large number of queries required. On the other hand, transferability-based attacks, despite their lower success rates on the target models, present a lower risk in terms of query overhead and perturbation efficiency, as demonstrated by their reduced L_0 and L_2 distances, especially when feature-importance-based selection is applied.

5.3. Attacker’s Effort

To assess the attacker’s effort, we compared the performance of the query- and transferability-based attacks in terms of the computational time, the required amount of data, and the computational resources needed (see Section 4.9).

With respect to the *computational time*, the attacker’s objective is to minimize the amount of time it takes to craft an adversarial sample. In query-based attacks, the computational time includes: *i*) the time it takes to query the target model (denoted as α); and *ii*) the time it takes to perform a single optimization iteration (denoted as β). The total amount of time it takes to craft an adversarial sample is calculated in Eq. (2):

$$Time(x, M) = nt^2\alpha\beta \quad (2)$$

where x is a data sample, M is the target model, n is the number of queries required to craft a successful adversarial sample, and t is the time it takes to perform a single query. When considering solely the query-related aspects of the

required time, query-based attacks are at a disadvantage compared to transferability-based attacks, since many more queries to the target model are required (see Section 5.2). However, in transferability-based attacks, there is another aspect to consider – the surrogate model’s training and querying time. The total amount of time it takes to craft an adversarial sample is calculated in Eq. (3), where we assume that the time it takes to perform a query to the target model is identical to the time required to perform a query to the surrogate model.

$$Time(x, M) = mt^2\alpha\beta + T_{surrogate} + t \quad (3)$$

where x is a data sample, M is the target model, m is the number of queries to the surrogate model required to craft a successful adversarial sample, and $T_{surrogate}$ is the time it takes to train the surrogate model. In transferability-based attacks that rely on an additional feature importance model, the total time must also include the time it takes to train that model.

In our evaluation, we found that the total amount of time it took to produce a single adversarial sample in query-based attacks was, on average, 518.4 seconds. However, in transferability-based attacks, it was ~ 243.5673 seconds: ~ 240.49 seconds to train the surrogate and feature importance models, 0.0773 seconds to generate the sample w the surrogate model, and ~ 3 seconds to query the target model. Based on this, we can conclude that although transferability-based attacks require training additional models, the total computational time required to craft a single adversarial sample is shorter than in query-based attacks.

With respect to the *amount of data* required, the attacker’s objective is to minimize the amount of data. In query-based attacks, the only data required by the attacker is the original sample that the adversarial sample will be based on, however in transferability-based attacks, the attacker must also possess a surrogate dataset to train the surrogate and feature importance models. Based on this, we can conclude that transferability-based attacks require more data samples than query-based attacks.

In our evaluation, the surrogate model was trained with the exact same amount of data used to train the target models (3,320, 62,848, and 33,727 samples from the Hate, ICU, and VideoTQ datasets respectively), and achieved satisfactory performance.

With respect to *computational resources*, the attacker’s objective is to minimize the amount of computational resources needed. In query-based attacks, the required resources include computational power for the adversarial sample generation process and storage to store the original and adversarial samples and the byproducts of the process (e.g., the target model’s response), which can be substantial when dealing with a large number of queries. In contrast, transferability-based attacks require the resources mentioned above, as well as additional storage and computational resources to train and store the surrogate and feature importance models. Based on this, we can conclude that

transferability-based attacks require more computational resources than query-based attacks.

In conclusion, while query-based attacks require less data, transferability-based attacks require less computational time and resources. However, they are limited by lower success rates compared to query-based attacks, as discussed in Section 5.2.

5.4. Attack Quality

In our evaluation, we assessed query- and transferability-based attacks in terms of the quality of the adversarial samples produced. This quality can be examined by considering both the adversarial sample’s coherence and its impact on the target model’s decision-making process. To measure the coherence of adversarial samples, we propose using metrics based on AE and IF models. To evaluate the impact on the target model’s decision-making process, we introduced two new metrics derived from the SHAP framework (see Section 4.9).

Feature Space Coherency. Fig. 3 presents the anomaly detection rates derived from the values obtained using the IF model and the reconstruction errors from the AE for adversarial samples for each evaluated attack, target class, and dataset. Each anomaly detection rate represents the percentage of adversarial samples identified as anomalies. For the AE, a sample is considered anomalous if its reconstruction error exceeds a predefined threshold (see Eq. (1)). The false positive rate (FPR) for benign samples, based on the specified threshold, is 0.020 and 0.011 for class 0 and class 1 on the Hate dataset, 0.038 and 0.038 on the ICU dataset, and 0.014 and 0.002 on the VideoTQ dataset. The same FPR was applied to the IF model for comparison.

On the Hate dataset, the boundary attack led to a 100% detection rate for adversarial samples for both target classes by both the AE and IF models. For the HopSkipJump attack, a 100% anomaly detection was obtained for adversarial samples in class 0 by both the AE and IF models when targeting the GB and LGB models; however, no anomalies were detected for adversarial samples in class 1 across all target models. This discrepancy may arise from HopSkipJump’s initial adversarial sample selection and the optimization process, i.e., selecting a sample from the target class that is closest to the original sample and increasing proximity to the original sample using gradient estimation, whereas the boundary attack uses a random initial adversarial sample from the target class and does not employ gradient estimation (see Appendix A). In the case of the transferability-based attacks, only the AE successfully detected anomalies, achieving a 100% anomaly detection rate for most attacks for both target classes.

On the ICU dataset, the boundary attack demonstrated similar performance trends as observed for the Hate dataset, however, the HopSkipJump attack resulted in fewer detected anomalies for both target classes across both the AE and IF models. The transferability-based attacks also led to significantly fewer anomalies, with the exception of the LGB importance-based (LGB imp.) and random-based selection

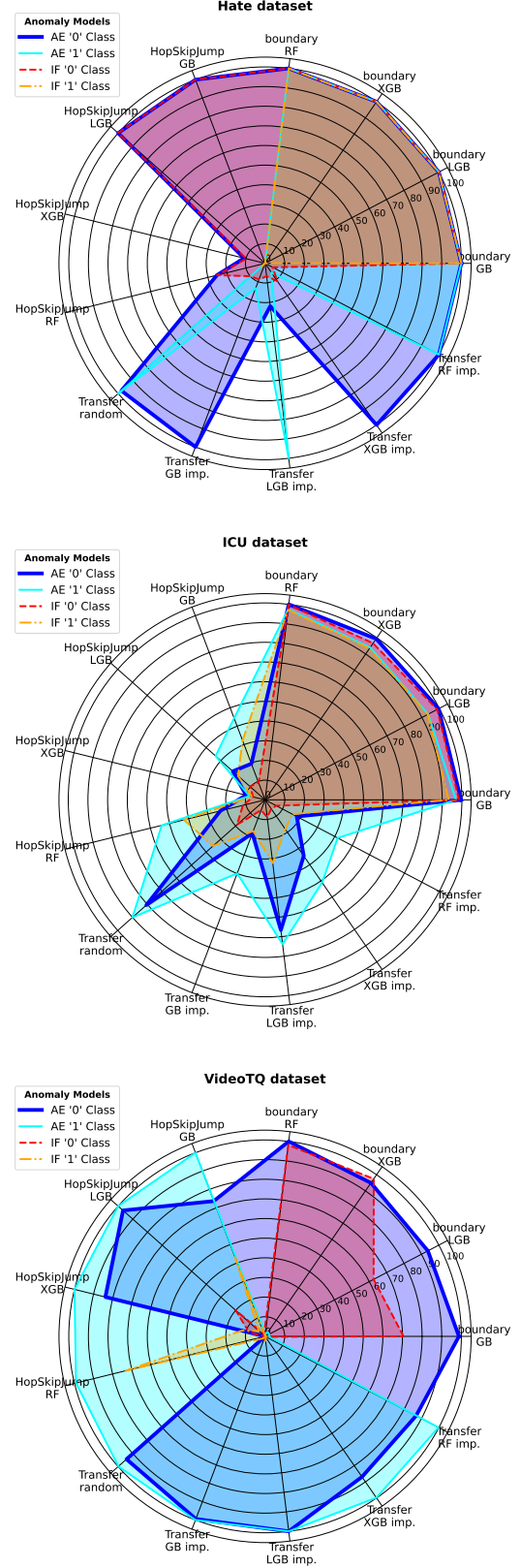


Figure 3: Attack quality evaluated based on the *anomaly detection rate* by AE and IF models across datasets, computed separately for each class. The FPR on all datasets for both classes is less than 0.04.

Table 4

Attack quality: results based on the *Importance-Based Anomaly Detection Rate* (percentage of samples with at least one feature with an anomalous SHAP value) and the *Average Anomalous SHAP Features per Sample* computed according to the features' SHAP values. **Bold** values are samples with the fewest changes in SHAP values, indicating high-quality samples in terms of having minimal impact on the target model's decision process.

Dataset	Target Model	Query Attacks		Transferability Attacks				
		boundary	HopSkipJump	random	GB imp.	LGB imp.	XGB imp.	RF imp.
		Importance-Based Anomaly Detection Rate (%) / Average Anomalous SHAP Features per Sample						
Hate	GB	100.0 / 7.7	96.7 / 5.6	100.0 / 8.4	100.0 / 8.9	81.2 / 3.3	27.3 / 0.4	25.6 / 0.5
	LGB	58.2 / 1.1	78.0 / 1.7	64.3 / 1.6	79.7 / 2.0	76.8 / 1.7	69.9 / 1.4	40.5 / 0.7
	XGB	26.4 / 0.4	67.6 / 1.1	86.4 / 1.8	92.1 / 1.9	80.3 / 1.6	22.0 / 0.3	24.8 / 0.3
	RF	63.2 / 1.0	30.8 / 0.5	100.0 / 3.8	100.0 / 4.2	75.7 / 3.4	67.3 / 0.9	50.0 / 0.6
ICU	GB	29.0 / 0.4	19.4 / 0.3	7.3 / 0.1	10.8 / 0.1	1.8 / 0.0	3.5 / 0.0	3.5 / 0.0
	LGB	4.1 / 0.0	3.9 / 0.0	22.3 / 0.2	17.5 / 0.2	2.4 / 0.0	6.9 / 0.1	5.6 / 0.1
	XGB	3.5 / 0.0	6.0 / 0.1	6.5 / 0.1	6.4 / 0.1	4.2 / 0.0	5.1 / 0.1	3.3 / 0.0
	RF	0.1 / 0.0	0.2 / 0.0	4.0 / 0.0	0.5 / 0.0	0.0 / 0.0	0.0 / 0.0	0.7 / 0.0
VideoTQ	GB	5.3 / 0.1	9.4 / 0.2	0.4 / 0.0	1.0 / 0.0	51.4 / 0.8	90.3 / 1.5	64.3 / 1.1
	LGB	7.3 / 0.1	1.5 / 0.0	3.4 / 0.0	3.4 / 0.0	0.8 / 0.0	0.6 / 0.0	1.0 / 0.0
	XGB	38.9 / 0.4	25.2 / 0.3	0.4 / 0.0	1.0 / 0.0	21.6 / 0.2	31.5 / 0.3	17.8 / 0.2
	RF	66.6 / 0.7	87.6 / 0.9	0.0 / 0.0	0.0 / 0.0	0.0 / 0.0	68.8 / 0.7	79.0 / 0.8

attacks. These two methods resulted in 60–90% of samples from both target classes being detected as anomalies by the AE model.

On the VideoTQ dataset, all attacks resulted in high anomaly detection rates (85–100%) by the AE model. Except for the boundary attack, which achieved a 0% anomaly detection rate for class 1 by both the AE and IF models.

As shown in Fig. 3, the two query-based attacks demonstrate distinct behaviors in terms of the models' anomaly detection rates. Most adversarial samples generated by the boundary attack were detected as anomalous by both models. In contrast, adversarial samples from the HopSkipJump attack, similar to those from transferability-based attacks, were consistently detected as anomalous only by the AE model.

Notably, despite the HopSkipJump and transferability-based attacks producing samples with lower L_2 distances (as detailed in Section 5.2, these samples were still identifiable as anomalous. This suggests that even subtle perturbations introduced by these attacks can still be identified as anomalous.

Model Interpretation Stability.

Figs. 4 to 6 presents the distribution of SHAP values for adversarial versus benign samples across different attacks and datasets for each target model. To simplify the presentation, we focus on the top-four most important features, selected based on their average SHAP values computed on the benign training dataset.

As shown in the figures, for most target models and datasets, there is at least one feature where the SHAP value distribution across attacks varies significantly. Analyzing the SHAP-based feature importance of a queried sample can therefore be an effective technique for identifying attacks.

Table 4 presents the results of our evaluation of attack quality using SHAP-based metrics. For each attack and target model, we report the Importance-Based Anomaly Detection Rate (percentage of samples with at least one anomalous feature based on SHAP values) and the Average Anomalous SHAP Features per Sample (as described in Section 4.9). Lower values indicate that there is less impact on the model's decision-making process, meaning that adversarial samples were more consistent with benign samples in terms of feature importance (i.e., the model relies on similar features for prediction).

On the Hate dataset, transferability-based attacks using XGB and RF feature importance techniques (referred to in the table as XGB imp. and RF imp.) resulted in lower importance-based anomaly detection rates and lower values of average anomalous SHAP features per sample compared to other transferability- and query-based attacks. The boundary attack on the XGB model and HopSkipJump attack on the RF model also resulted in both a low importance-based anomaly detection rate and a low average number of anomalous features per sample. This indicates that the changes to feature importance were less distinguishable for those attacks.

On the ICU dataset, both query- and transferability-based attacks generally produced less anomalous SHAP values for most target models (LGB, XGB, and RF), with importance-based anomaly detection rates typically below 7% and very low values of average anomalous SHAP features per sample ranging from 0.0 to 0.1. However, when targeting the GB model, transferability-based attacks resulted in notably lower importance-based anomaly detection rates (1.8% to 10.8%) compared to query-based attacks (29.0% and 19.4% for the boundary and HopSkipJump attacks, respectively). In this case, the average number of anomalous

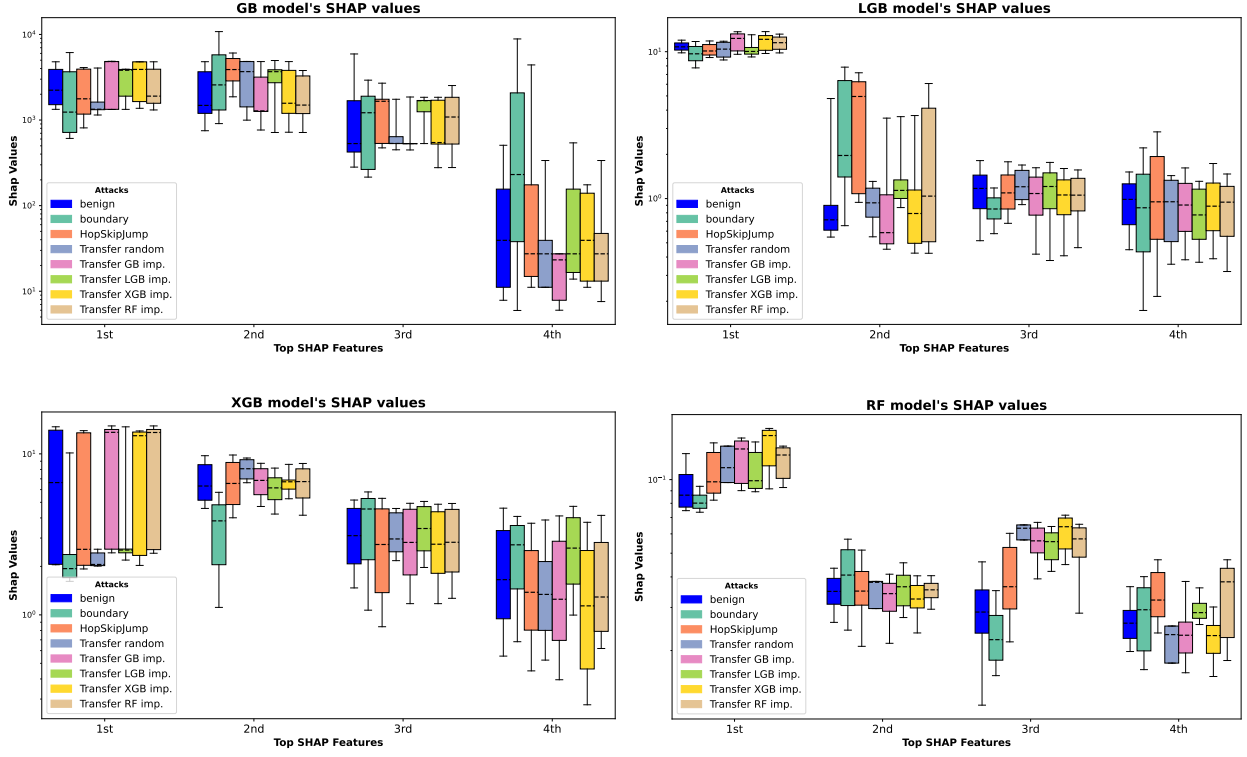


Figure 4: Attack quality evaluated based on the impact on the target model's decision-making process; SHAP value distribution for benign (blue) and adversarial samples (on the **Hate dataset**), across the top-four most important features selected based on their average SHAP values computed on the benign training dataset.

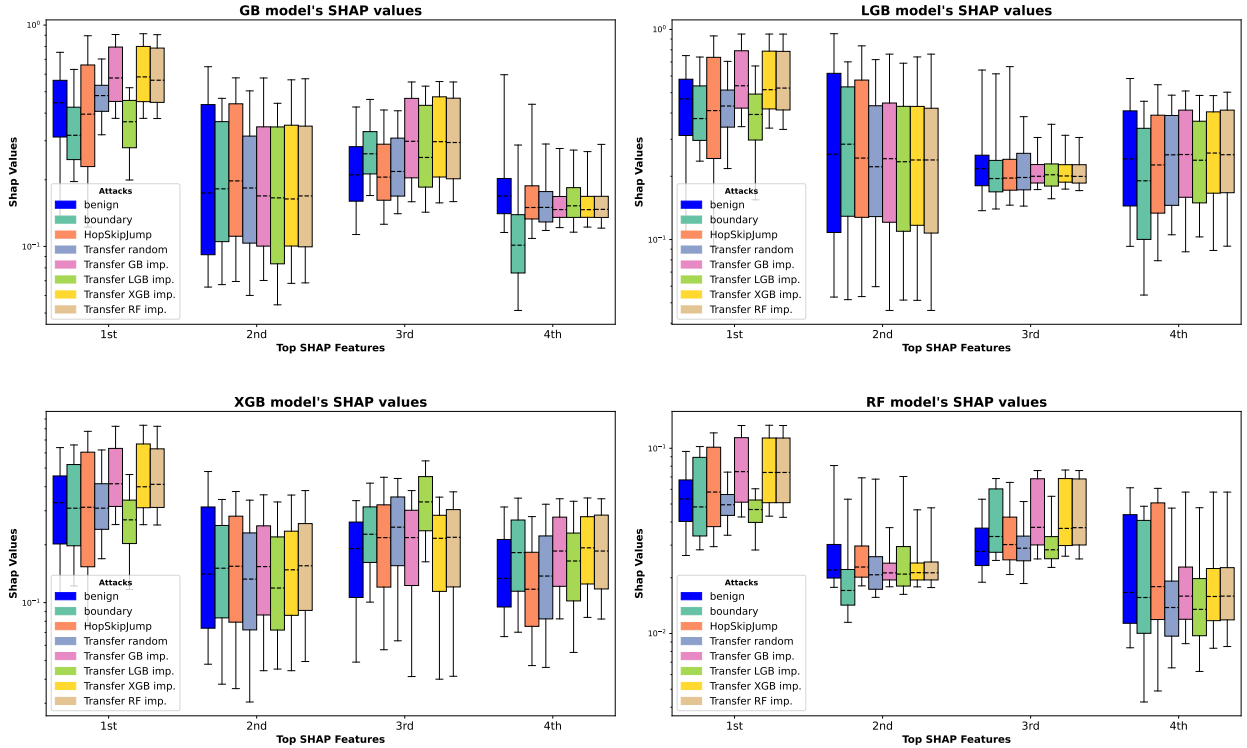


Figure 5: Attack quality evaluated based on the impact on the target model's decision-making process; SHAP value distribution for benign (blue) and adversarial samples (on the **ICU dataset**), across the top-four most important features selected based on their average SHAP values computed on the benign training dataset.

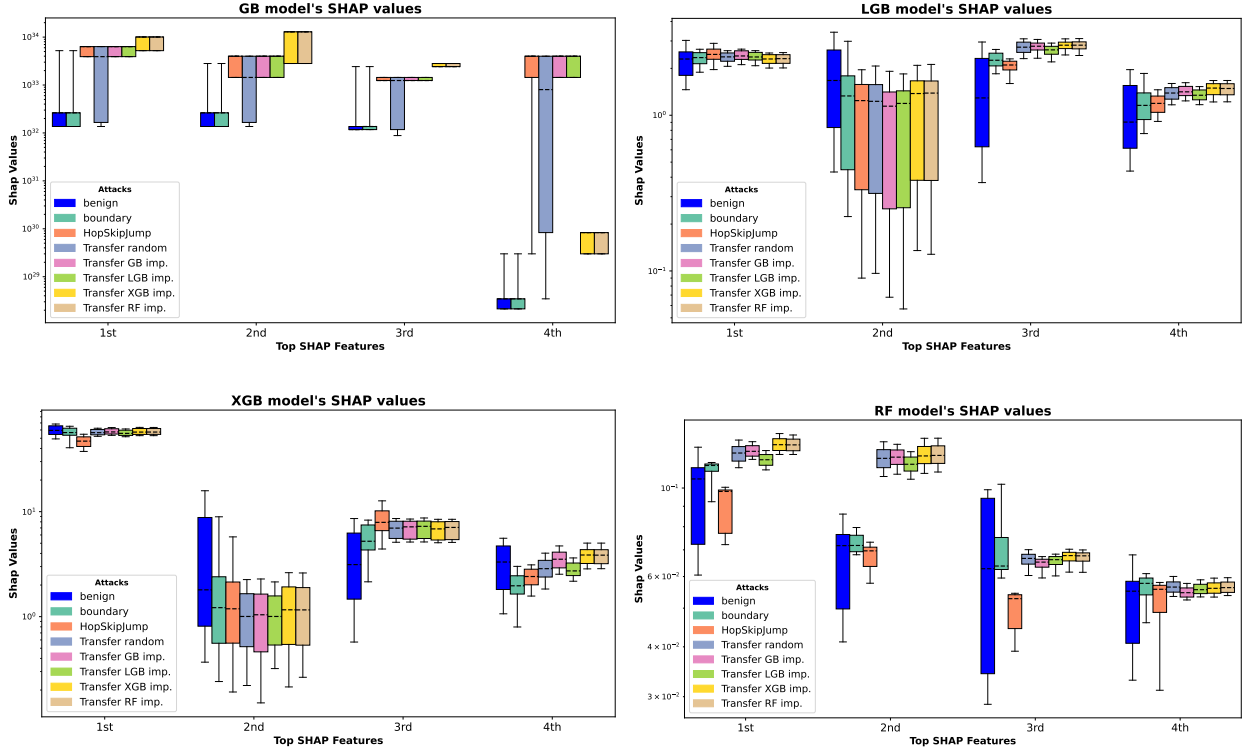


Figure 6: Attack quality evaluated based on the impact on the target model’s decision-making process; SHAP value distribution for benign (blue) and adversarial samples (on the **VideoTQ** dataset), across the top-four most important features selected based on their average SHAP values computed on the benign training dataset.

SHAP features per sample was slightly higher for query-based attacks (0.3 to 0.4) than for transferability-based attacks (0.0 to 0.1), though still relatively low overall.

On the VideoTQ dataset, transferability-based attacks resulted in less anomalous SHAP values than query-based attacks in most cases, specifically for the GB imp., LGB imp., and RF imp. feature importance techniques, where most transferability attacks resulted in importance-based anomaly detection rates below 1%. Notably, for the GB target model, both query-based attacks resulted in lower anomalous SHAP values (5.3% and 9.4% for boundary and HopSkipJump, respectively), while some transferability-based attacks resulted in higher importance-based anomaly detection rates (51.4%, 90.3%, and 64.3% for GB imp., LGB imp., and RF imp., respectively). All attacks resulted in very few anomalous SHAP features per sample, and in most cases, the number of anomalous features per sample was close to 0.0.

Based on the results in the table, we conclude that while the examined transferability-based attacks were designed to craft subtle and well-suited perturbations and generally result in a low importance-based anomaly detection rate, they do not always outperform query-based methods in generating coherent and consistent adversarial samples. Their effectiveness depends on several key factors, including the importance-based selection method used (i.e., the model from which feature importance is computed),

dataset-specific constraints and characteristics, and the target model’s architecture.

In highly constrained datasets like the ICU dataset where many features cannot be modified and over 30% of the features are categorical, transferability attacks tend to produce perturbations of similar magnitude to query-based attacks on categorical features, making query-based approaches competitive in these scenarios. The limited number of editable features forces both query- and transferability-based attacks to make fewer changes, causing less anomalous behavior overall. The random-based selection attack is an exception, as it compromises coherence by arbitrarily modifying features, often resulting in anomalous values and noticeable changes in SHAP values.

These findings suggest that defense mechanisms should consider not only the attack strategy but also the specific dataset and model vulnerabilities.

Our evaluation of attack quality—employing both the anomaly detection rate to assess sample coherence and the importance-based anomaly detection rate to evaluate the impact of adversarial samples on the target model’s decision-making process—reveals complementary insights. The Importance-Based Anomaly Detection Rate (computed based on SHAP values, see Table 4), can help identify adversarial samples that appear normal when evaluating just their feature values. For example, on the Hate dataset, the HopSkipJump attack only produced anomalous values when

Table 5

CSAD versus standard approach. The standard approach compares adversarial samples to all benign samples regardless of class, while CSAD only compares adversarial samples to benign samples of the same predicted class. Higher values indicate better detection results.

Dataset	Target Model	Query Attacks		Transferability Attacks				
		boundary	HopSkipJump	random	GB imp.	LGB imp.	XGB imp.	RF imp.
		Standard Approach (%) / Class-Specific Anomaly detection (CSAD) Approach (%)						
Hate	GB	87.9 / 100.0	64.1 / 96.7	94.4 / 100.0	96.7 / 100.0	100.0 / 81.2	10.0 / 27.3	32.0 / 25.6
	LGB	8.6 / 58.2	40.4 / 78.0	52.6 / 64.3	50.0 / 79.7	20.0 / 76.8	22.0 / 69.9	28.6 / 40.5
	XGB	0.0 / 26.4	6.6 / 67.6	70.3 / 86.4	56.0 / 92.1	50.0 / 80.3	4.5 / 22.0	13.6 / 24.8
	RF	37.9 / 63.2	23.5 / 30.8	62.6 / 100.0	74.0 / 100.0	75.0 / 75.7	37.8 / 67.3	20.0 / 50.0
ICU	GB	8.4 / 29.0	5.1 / 19.4	0.3 / 7.3	1.2 / 10.8	0.6 / 1.8	0.9 / 3.5	1.2 / 3.5
	LGB	1.0 / 4.1	1.2 / 3.9	3.8 / 22.3	4.1 / 17.5	0.9 / 2.4	4.3 / 6.9	4.5 / 5.6
	XGB	2.6 / 3.5	3.9 / 6.0	1.0 / 6.2	2.2 / 6.4	0.0 / 4.2	4.2 / 5.1	3.3 / 3.3
	RF	0.0 / 0.1	0.0 / 0.2	0.0 / 4.0	0.0 / 0.5	0.0 / 0.0	0.0 / 0.0	0.0 / 0.7
VideoTQ	GB	1.2 / 5.3	0.7 / 9.4	0.0 / 0.4	0.8 / 1.0	43.8 / 51.4	90.2 / 90.3	64.3 / 64.3
	LGB	6.7 / 7.3	0.0 / 1.5	4.1 / 3.4	10.6 / 3.4	0.8 / 0.8	1.0 / 0.6	0.8 / 1.0
	XGB	47.0 / 38.9	21.4 / 25.2	0.0 / 0.4	0.9 / 1.0	21.9 / 21.6	30.9 / 31.5	17.2 / 17.8
	RF	0.0 / 66.6	0.0 / 87.6	13.8 / 0.0	17.0 / 0.0	0.0 / 0.0	0.0 / 68.8	0.0 / 79.0

performed against the GB and LGB target models (see Section 5.4). However, when evaluating anomalies in SHAP values, our proposed metric captured anomalies when attacking the XGB and RF target models as well (see Table 4). On the VideoTQ dataset, we observed the opposite phenomenon; here, traditional anomaly detection (specifically using the AE model) captured anomalies for all of the transferability-based attacks (see Section 5.4), while the SHAP values were not anomalous in many cases (see Table 4).

These contrasting results underscore the importance of considering anomaly detection rates based on both sample values and feature importance when assessing the impact of adversarial attacks on model robustness. Each approach captures different aspects of adversarial perturbation, providing a more comprehensive understanding of the attack quality and potential defensive strategies.

5.5. Effectiveness of the Class-Specific Anomaly Detection (CSAD) Approach

Table 5 presents the results of two approaches for computing the anomaly detection rate: (1) the CSAD approach, which measures the anomalousness of SHAP values in adversarial samples in relation to benign SHAP values of the same predicted class only, and (2) the standard approach, which compares adversarial samples to the entire benign SHAP value distribution across all classes, enabling a comparative analysis of detection effectiveness between class-specific and general anomaly detection methods.

For each attack and target model, the table presents the percentage of samples with at least one anomalous feature based on SHAP values using both approaches. Higher values indicate greater success in detecting compromised adversarial samples. For each pair of results, the approach with the better detection rate is highlighted in bold. The results demonstrate that the CSAD approach substantially improves the detection of adversarial samples in most cases, often

achieving a detection rate that is over twice that of the standard approach. Particularly notable are cases involving the RF target model on the VideoTQ dataset, where the CSAD approach achieved detection rates of 66.6% and 87.6% for the boundary and HopSkipJump attacks respectively, compared to 0% detection with the standard approach.

These findings confirm that assessing anomalies in data samples with respect to their specific target class is essential, particularly when the data distribution across features is not uniform. By comparing adversarial samples to benign samples of the same class, the CSAD approach accounts for class-specific patterns, leading to improved anomaly detection. This approach is especially valuable for datasets in which the normal patterns in the features of the classes differ. Subtle changes that only matter for specific classes may go undetected when a global threshold for all classes is used.

6. Discussion

The results from our evaluation of the attacker’s risk highlight the trade-offs between different attack strategies. The examined query-based attacks achieved near-perfect success rates (often exceeding 98%). However, this consistency comes at the cost of larger distortions and high computational overhead that is reflected in increased L_0 and L_2 distances. Transferability-based approaches offered efficiency advantages but struggled with success rates, particularly on complex datasets like the ICU dataset. The lower attack success rates for transferability-based attacks on the evaluated datasets highlight their limitations in adversarial scenarios. Importantly, when defenders rely on query-based attacks as part of defense strategies (e.g., adversarial training), it is crucial to recognize that such attacks may not capture the same degree of feature coherence exhibited

by transferability-based attacks, potentially leaving gaps in robustness.

On datasets with a limited number of editable features like ICU and VideoTQ, transferability attacks struggled more in terms of success rate than the more flexible Hate dataset which has a high number of editable features. However, from a defender’s perspective, transferability-based attacks present a unique challenge. Despite their lower overall success rate, when adversarial samples generated by these attacks do succeed in deceiving the target model, they may evade traditional detection mechanisms, underscoring the complexity of defending against these types of attacks.

Interestingly, while small L_2 distances are commonly regarded in the literature as indicative of imperceptibility, our findings suggest this may not hold for tabular data. In some cases, transferability-based attacks that achieved very small L_2 distances were still detected as anomalies by the AE. This finding calls into question the assumption that lower L_2 norm correlate with indistinguishability in tabular data domains, where imperceptibility may depend on other factors besides the L_2 distance.

Our comprehensive evaluation, which assessed both feature space coherency and the stability of model interpretation (via SHAP), showed that adversarial perturbations can affect feature values and model interpretations independently. Some attacks (like the HopSkipJump attack when targeting XGB and RF models on the Hate dataset) preserved normal feature distributions in the sample values while significantly altering the model’s decision-making as reflected in the anomalous SHAP values. Others (like several transferability-based attacks on the VideoTQ dataset) showed the opposite pattern with anomalous sample values but relatively normal SHAP distributions. This finding suggests that comprehensive defense systems should monitor both the raw feature values and their impact on model decision-making, since focusing solely on one could cause sophisticated attacks targeting the other to go undetected.

The superiority of the CSAD approach seen in our evaluation demonstrates that context-specific thresholds substantially outperform global thresholds for identifying adversarial samples. This finding likely extends beyond our specific implementation to other defense mechanisms, where class-conditional modeling could improve detection accuracy.

Regarding anomaly detection models, the neural network-based AE detector identified more adversarial samples as anomalous than the tree-based IF alternative (as expected). These empirical results validate that AEs better capture the complex patterns and relationships in the data, making them more sensitive to subtle adversarial manipulations in tabular datasets.

7. Conclusion

In this study we compared effectiveness of different black-box adversarial attacks strategies on ML models for tabular data. Our evaluation framework considers the attacker’s risk, effort, and the quality of adversarial samples,

providing insights for both attack optimization and defense strategies.

The results obtained using diverse target models and datasets highlight distinct trade-offs: query-based attacks, while highly effective, often sacrifice coherence by causing significant distortions, and require substantial computational resources. Transferability-based attacks, though less successful in some cases, achieve greater coherence and consistency with fewer feature modifications, resulting in subtler impact on model decision-making. This is evidenced by lower anomaly detection rates and minimal changes in feature importance.

Designing adversarial attacks for tabular data thus requires balancing sample coherence and the attack success rate. This balance is especially important in the context of query-based attacks, particularly when these attacks are used by defenders as part of adversarial training. To support the necessary balancing, we introduced novel metrics for assessing those aspects of adversarial samples and attacks in the tabular domain. These metrics independently capture anomalies in both feature space values and model interpretation (as reflected in SHAP values), representing the surface-level coherence of samples as well as their internal impact on the model’s decision-making process. Our evaluation framework, which combines traditional anomaly detection with SHAP-based analysis, demonstrates that perturbations can independently affect each of these aspects. This underscores the importance of monitoring both aspects when designing or defending against adversarial attacks.

Furthermore, Our CSAD approach, which employs context-specific thresholds, markedly improved detection rates over approaches that utilize a global threshold, emphasizing the importance of examining class-specific patterns in identifying adversarial samples.

These findings and metrics lay the groundwork for future research, enabling the development of more balanced attack strategies that maximize effectiveness while preserving feature space coherency. This, in turn, can help defenders bolster their systems against such threats.

Future work could investigate adversarial robustness in more complex tabular ML pipelines, including scenarios where models incorporate built-in defenses against such attacks or where attackers does not have full knowledge of the target model’s features. By building on the insights and methodologies presented here, researchers can further refine both attack and defense strategies in the tabular domain.

8. Declarations

The authors declare that they have no known competing financial interests or personal relationships that could have appeared to influence the work reported in this paper.

Appendix A Pseudocode for Tabular Attacks

In this research, we applied two types of query-based attacks: the Boundary and HopSkipJump attacks, along with

five versions of transferability-based attack, all adapted for the tabular domain and outlined below.

In the Boundary attack presented in Algorithm 1, the attacker randomly selects a sample from the defined target class, regardless of its proximity to the original sample (lines 2-3). The attacker then optimizes the modified sample's values using an orthogonal perturbation, which iteratively adjusts the feature values to minimize the model's confidence in the original class while ensuring that the predicted class is the target class (lines 4-6). During the crafting process, tabular constraints are applied to the sample (see Algorithm 2), projecting each feature value onto its closest legitimate value to ensure input validity (line 7).

Algorithm 1: The Boundary adversarial attack for tabular data

Input: The target model M , original sample x , original sample's true label y , set of immutable features I , set of each feature constraints $Constraints$, and the similarity threshold α

```

1  $x^{adv} \leftarrow x$ 
2 while  $i < max\_init\_steps \wedge M(x^{adv}) = y$  do
3    $x^{adv} \leftarrow$  random perturbation from distribution
    $x \sim \mathcal{N}(\mu, \sigma^2)$ 
end
4 while  $i < max\_iteration\_steps \wedge M(x^{adv}) = y \wedge$ 
    $Similarity(x, x^{adv}) < \alpha$  do
5   while  $j < max\_similarity\_steps$  do
6      $x^{adv} \leftarrow x^{adv} +$ 
       Orthogonal_Perturbation( $x, x^{adv}$ )
   end
7    $x^{adv} \leftarrow$  Tabular_Modify( $x, x^{adv}, I, Constraints,$ 
     regression_models)
end
8 return  $x^{adv}$ 

```

Algorithm 2: A generic procedure for applying constraints of tabular data domains

Input: The original sample x , adversarial sample x^{adv} , set of immutable features I , and the set of each feature constraints $Constraints$

```

1 Procedure Tabular_Modify( $x, x^{adv}, I, Constraints,$ 
  regression_models)
2   Clip (min, max)
3   Impose realistic values (constraints)
4   Impose immutable features ( $I$ )
5   Correct dependent features (regression_models)
6   return adversarial

```

In contrast, in the HopSkipJump attack, which is presented in Algorithm 3, the attacker employs binary search and proceeds in the target class gradients' direction to find a sample from the defined target class with the closest

proximity to the original sample (lines 5-10). During the binary search, tabular constraints are applied to the sample (see Algorithm 2), projecting each feature value onto its closest legitimate value to ensure input validity (line 11).

Algorithm 3: The HopSkipJump adversarial attack for tabular data

Input: The target model M , original sample x , original sample's true label y , set of immutable features I , set of each feature constraints $Constraints$, and the similarity threshold α

```

1  $x^{adv} \leftarrow x$ 
2 while  $i < max\_init\_steps \wedge M(x^{adv}) = y$  do
3    $x^{adv} \leftarrow$  random perturbation from distribution
    $x \sim \mathcal{N}(\mu, \sigma^2)$ 
4    $x^{adv} \leftarrow$  Binary_Search( $x, x^{adv}$ )
end
5 while  $i < max\_iteration\_steps \wedge M(x^{adv}) = y \wedge$ 
    $Similarity(x, x^{adv}) < \alpha$  do
6   while  $j < max\_similarity\_steps$  do
7      $x^{adv} \leftarrow$  Binary_Search( $x, x^{adv}$ )
8      $update \leftarrow$  Compute_Update( $x, x^{adv}$ )
9      $potential\_sample \leftarrow$  run step size search
       ( $x^{adv}, update$ ) until predicts satisfying
10     $x^{adv} \leftarrow potential\_sample$ 
  end
11   $x^{adv} \leftarrow$  Tabular_Modify( $x, x^{adv}, I, Constraints$ )
end
12 return  $x^{adv}$ 

```

In our evaluation, we implemented untargeted transferability-based gradient attacks based on the architecture in [36, 21], and the pseudocode is presented in Algorithm 4. The attacker first selects the feature likely to have the most impact on the model's prediction, excluding immutable features, i.e., features that cannot be changed by the attacker (line 4). The selection, which is presented in lines 9-13, can be made by: 1) selecting k random features and the n features that are most correlated with them [36]. 2-4) using a feature importance technique to select the k most important features [21] and the n features that are most correlated with them. The feature importance technique can be performed by training an ML classifier (such as GB, XGB, LGB, and RF models) and extracting what they consider the most important features [21]. After selecting features to perturb, a perturbation vector p is calculated for the selected features by using an optimizer that minimizes the adversary's objective function (line 5). Finally, tabular constraints are applied to the sample (see Algorithm 2), projecting each feature value onto its closest legitimate value to ensure input validity (line 7).

Algorithm 4: An untargeted transferability-based adversarial attack for tabular data

Input: The target model M , original sample x , original sample's true label y , adversary's objective loss function L^{adv} , set of immutable features I , set of each feature constraints $Constraints$, maximum allowed L_0 -perturbation noise λ , number of most important features to perturb k , and number of features most correlated with the k features chosen n

```
1  $x^{adv} \leftarrow x$ 
2  $F \leftarrow \emptyset$ 
3 while  $M'(x^{adv}) = y \wedge |F| < \lambda$  do
4    $F \leftarrow F \cup \text{Select\_Features}(M', x^{adv}, I, F, k, n)$ 
5    $p \leftarrow \text{Compute\_Perturbation}(M', L^{adv}, x^{adv}, F)$ 
6    $x_i^{adv} \leftarrow x_i^{adv} + p$ 
7    $x^{adv} \leftarrow$ 
      $\quad \text{Tabular\_Modify}(x, x^{adv}, I, Constraints)$ 
8 return  $x^{adv}$ 

Procedure  $\text{Select\_Features}(M', x^{adv}, I, F, k, n)$ 
9   •Random-Based Selection
10  •GB Feature Importance-Based Selection
11  •XGB Feature Importance-Based Selection
12  •LGB Feature Importance-Based Selection
13  •RF Feature Importance-Based Selection
```

CRedit authorship contribution statement

Yael Itzhakev: Writing – review & editing, Writing – original draft, Visualization, Data curation, Investigation, Formal analysis, Validation, Software, Methodology, Conceptualization. **Amit Giloni:** Writing – review & editing, Validation, Conceptualization. **Yuval Elovici:** Supervision. **Asaf Shabtai:** Supervision, Project administration.

References

- [1] Alecci, M., Conti, M., Marchiori, F., Martinelli, L., Pajola, L., 2023. Your attack is too dumb: Formalizing attacker scenarios for adversarial transferability, in: Proceedings of the 26th International Symposium on Research in Attacks, Intrusions and Defenses, pp. 315–329.
- [2] Ballet, V., Renard, X., Aigrain, J., Laugel, T., Frossard, P., Detyniecki, M., 2019. Imperceptible adversarial attacks on tabular data. arXiv preprint arXiv:1911.03274 .
- [3] Belle, V., Papantonis, I., 2021. Principles and practice of explainable machine learning. Frontiers in big Data , 39.
- [4] Borisov, V., Leemann, T., Seßler, K., Haug, J., Pawelczyk, M., Kasneci, G., 2022. Deep neural networks and tabular data: A survey. IEEE transactions on neural networks and learning systems .
- [5] Breiman, L., 2001. Random forests. Machine learning 45, 5–32.
- [6] Brendel, W., Rauber, J., Bethge, M., 2017. Decision-based adversarial attacks: Reliable attacks against black-box machine learning models. arXiv preprint arXiv:1712.04248 .
- [7] Byun, J., Go, H., Kim, C., 2022. On the effectiveness of small input noise for defending against query-based black-box attacks, in: Proceedings of the IEEE/CVF Winter Conference on Applications of Computer Vision, pp. 3051–3060.
- [8] Cartella, F., Anunciacao, O., Funabiki, Y., Yamaguchi, D., Akishita, T., Elshocht, O., 2021. Adversarial attacks for tabular data: Application to fraud detection and imbalanced data. arXiv preprint arXiv:2101.08030 .
- [9] Chen, J., Jordan, M.I., Wainwright, M.J., 2020. Hopskipjumpattack: A query-efficient decision-based attack, in: 2020 IEEE Symposium on Security and Privacy (SP), IEEE. pp. 1277–1294.
- [10] Chen, T., Guestrin, C., 2016. Xgboost: A scalable tree boosting system, in: Proceedings of the 22nd ACM SIGKDD International Conference on Knowledge Discovery and Data Mining, pp. 785–794.
- [11] Chen, X., Liu, C., Zhao, Y., Jia, Z., Jin, G., 2022. Improving adversarial robustness of bayesian neural networks via multi-task adversarial training. Information Sciences 592, 156–173.
- [12] Crouhy, M., Galai, D., Mark, R., 2000. A comparative analysis of current credit risk models. Journal of Banking & Finance 24, 59–117.
- [13] Danese, M.D., Halperin, M., Duryea, J., Duryea, R., 2019. The generalized data model for clinical research. BMC medical informatics and decision making 19, 1–13.
- [14] Deldjoo, Y., Noia, T.D., Merra, F.A., 2021. A survey on adversarial recommender systems: from attack/defense strategies to generative adversarial networks. ACM Computing Surveys (CSUR) 54, 1–38.
- [15] Fezza, S.A., Bakhti, Y., Hamidouche, W., Déforges, O., 2019. Perceptual evaluation of adversarial attacks for cnn-based image classification, in: 2019 Eleventh International Conference on Quality of Multimedia Experience (QoMEX), IEEE. pp. 1–6.
- [16] Fisher, R.A., Fisher, R.A., 1971. The design of experiments. Springer.
- [17] Friedman, J.H., 2001. Greedy function approximation: a gradient boosting machine. Annals of statistics , 1189–1232.
- [18] Gómez, A.L.P., Maimó, L.F., Celdrán, A.H., Clemente, F.J.G., 2023. Vaasi: Crafting valid and abnormal adversarial samples for anomaly detection systems in industrial scenarios. Journal of Information Security and Applications 79, 103647.
- [19] Goodfellow, I.J., Shlens, J., Szegedy, C., 2014. Explaining and harnessing adversarial examples. arXiv preprint arXiv:1412.6572 .
- [20] Goyal, S., Doddapaneni, S., Khapra, M.M., Ravindran, B., 2023. A survey of adversarial defenses and robustness in nlp. ACM Computing Surveys 55, 1–39.
- [21] Grolman, E., Binyamini, H., Shabtai, A., Elovici, Y., Morikawa, I., Shimizu, T., 2022. Hateversarial: Adversarial attack against hate speech detection algorithms on twitter, in: Proceedings of the 30th ACM Conference on User Modeling, Adaptation and Personalization, pp. 143–152.
- [22] Hanberger, H., Monnet, D.L., Nilsson, L.E., 2005. Intensive care unit, in: Antibiotic policies: theory and practice. Springer, pp. 261–279.
- [23] Haroon, M.S., Ali, H.M., 2022. Adversarial training against adversarial attacks for machine learning-based intrusion detection systems.

Computers, Materials & Continua 73.

- [24] Ilyas, A., Engstrom, L., Athalye, A., Lin, J., 2018. Black-box adversarial attacks with limited queries and information, in: International conference on machine learning, PMLR. pp. 2137–2146.
- [25] Ju, L., Cui, R., Sun, J., Li, Z., 2022. A robust approach to adversarial attack on tabular data for classification algorithm testing, in: 2022 8th International Conference on Big Data and Information Analytics (BigDIA), IEEE. pp. 371–376.
- [26] Kaviani, S., Han, K.J., Sohn, I., 2022. Adversarial attacks and defenses on ai in medical imaging informatics: A survey. *Expert Systems with Applications* 198, 116815.
- [27] Ke, G., Meng, Q., Finley, T., Wang, T., Chen, W., Ma, W., Ye, Q., Liu, T.Y., 2017. Lightgbm: A highly efficient gradient boosting decision tree. *Advances in neural information processing systems* 30.
- [28] Kingma, D.P., Ba, J., 2014. Adam: A method for stochastic optimization. *arXiv preprint arXiv:1412.6980*.
- [29] Kurakin, A., Goodfellow, I.J., Bengio, S., 2018. Adversarial examples in the physical world, in: Artificial intelligence safety and security. Chapman and Hall/CRC, pp. 99–112.
- [30] Lam, J.C., Wan, K.K., Cheung, K., Yang, L., 2008. Principal component analysis of electricity use in office buildings. *Energy and buildings* 40, 828–836.
- [31] Lan, J., Zhang, R., Yan, Z., Wang, J., Chen, Y., Hou, R., 2022. Adversarial attacks and defenses in speaker recognition systems: A survey. *Journal of Systems Architecture* 127, 102526.
- [32] Liu, L., Qi, H., 2017. Learning effective binary descriptors via cross entropy, in: 2017 IEEE winter conference on applications of computer vision (WACV), IEEE. pp. 1251–1258.
- [33] Lundberg, S.M., Lee, S.I., 2017. A unified approach to interpreting model predictions. *Advances in neural information processing systems* 30.
- [34] Mahmood, K., Mahmood, R., Rathbun, E., van Dijk, M., 2021. Back in black: A comparative evaluation of recent state-of-the-art black-box attacks. *IEEE Access* 10, 998–1019.
- [35] Marulli, F., Verde, L., Campanile, L., 2021. Exploring data and model poisoning attacks to deep learning-based nlp systems. *Procedia Computer Science* 192, 3570–3579.
- [36] Mathov, Y., Levy, E., Katzir, Z., Shabtai, A., Elovici, Y., 2022. Not all datasets are born equal: On heterogeneous tabular data and adversarial examples. *Knowledge-Based Systems* 242, 108377.
- [37] Moro, S., Laureano, R., Cortez, P., 2011. Using data mining for bank direct marketing: An application of the crisp-dm methodology.
- [38] Nicolae, M.I., Sinn, M., Tran, M.N., Buesser, B., Rawat, A., Wistuba, M., Zantedeschi, V., Baracaldo, N., Chen, B., Ludwig, H., et al., 2018. Adversarial robustness toolbox v1. 0.0. *arXiv preprint arXiv:1807.01069*.
- [39] Papernot, N., McDaniel, P., Goodfellow, I., Jha, S., Celik, Z.B., Swami, A., 2017. Practical black-box attacks against machine learning, in: Proceedings of the 2017 ACM on Asia conference on computer and communications security, pp. 506–519.
- [40] Papernot, N., McDaniel, P., Jha, S., Fredrikson, M., Celik, Z.B., Swami, A., 2016. The limitations of deep learning in adversarial settings, in: 2016 IEEE European symposium on security and privacy (EuroS&P), IEEE. pp. 372–387.
- [41] Pennington, J., Socher, R., Manning, C.D., 2014. Glove: Global vectors for word representation, in: Proceedings of the 2014 conference on empirical methods in natural language processing (EMNLP), pp. 1532–1543.
- [42] Puttagunta, M.K., Ravi, S., Nelson Kennedy Babu, C., 2023. Adversarial examples: attacks and defences on medical deep learning systems. *Multimedia Tools and Applications*, 1–37.
- [43] Ramesh, T., Prakash, R., Shukla, K., 2010. Life cycle energy analysis of buildings: An overview. *Energy and buildings* 42, 1592–1600.
- [44] Ribeiro, M., Calais, P., Santos, Y., Almeida, V., Meira Jr, W., 2018. Characterizing and detecting hateful users on twitter, in: Proceedings of the International AAAI Conference on Web and Social Media.
- [45] Sakurada, M., Yairi, T., 2014. Anomaly detection using autoencoders with nonlinear dimensionality reduction, in: Proceedings of the MLSDA 2014 2nd workshop on machine learning for sensory data analysis, pp. 4–11.
- [46] Sun, L., Dou, Y., Yang, C., Zhang, K., Wang, J., Philip, S.Y., He, L., Li, B., 2022. Adversarial attack and defense on graph data: A survey. *IEEE Transactions on Knowledge and Data Engineering*.
- [47] Szegedy, C., Zaremba, W., Sutskever, I., Bruna, J., Erhan, D., Goodfellow, I., Fergus, R., 2013. Intriguing properties of neural networks. *arXiv preprint arXiv:1312.6199*.
- [48] Wang, Q., Zheng, B., Li, Q., Shen, C., Ba, Z., 2020. Towards query-efficient adversarial attacks against automatic speech recognition systems. *IEEE Transactions on Information Forensics and Security* 16, 896–908.
- [49] Weisstein, E.W., 2006. Correlation coefficient. <https://mathworld.wolfram.com/>.
- [50] Xu, H., Ma, Y., Liu, H.C., Deb, D., Liu, H., Tang, J.L., Jain, A.K., 2020. Adversarial attacks and defenses in images, graphs and text: A review. *International Journal of Automation and Computing* 17, 151–178.
- [51] Xu, H., Pang, G., Wang, Y., Wang, Y., 2023. Deep isolation forest for anomaly detection. *IEEE Transactions on Knowledge and Data Engineering* 35, 12591–12604.
- [52] Zizzo, G., Hankin, C., Maffei, S., Jones, K., 2019. Adversarial machine learning beyond the image domain, in: Proceedings of the 56th Annual Design Automation Conference 2019, pp. 1–4.